

# Self-Diffusion of Three-Armed Star and Linear Polybutadienes and Polystyrenes in Tetrachloromethane Solution

Ernst von Meerwall,<sup>\*1a</sup> David H. Tomich,<sup>1a</sup> James Grigsby,<sup>1a</sup>  
Robert W. Pennisi,<sup>1b</sup> Lewis J. Fetters,<sup>1b</sup> and Nikos Hadjichristidis<sup>1c</sup>

Department of Physics and The Institute of Polymer Science, University of Akron, Akron, Ohio 44325, and Department of Industrial Chemistry, University of Athens, Athens (144), Greece. Received September 21, 1982

**ABSTRACT:** We have used the pulsed-gradient spin-echo method to measure the self-diffusion of linear and three-armed star-branched polystyrenes and polybutadienes ( $3 \times 10^3 \leq M \leq 10^6$ ) dissolved in  $\text{CCl}_4$  at 50 °C. We detect no evidence of cooperative diffusion in the semidilute regime. The polymer diffusivities at infinite dilution obey Flory's theory, while their concentration dependences in the dilute regime follow a Pyun-Fixman model. No differences between linear and three-armed molecules are observed in this experiment.

## Introduction

The rheological properties of polymers have over the years attracted considerable experimental and theoretical attention. Of particular interest are dilute<sup>2-6</sup> and semidilute<sup>7,8</sup> solutions, the former to characterize the expansion of individual chain molecules and the latter to study their mutual interactions.

Self-diffusion measurements are useful in this respect both to complement intrinsic viscosity studies and in their own right, since friction coefficients seem to depend relatively sensitively on their experimental definition.<sup>9</sup> The pulsed-gradient spin-echo (PGSE) method for measuring self-diffusion<sup>10</sup> is now well established and has already yielded useful information in dilute polymer solutions.<sup>11,12</sup> Provided that the product of diffusion coefficient and the time scale of the measurement is sufficiently great, the method measures only Brownian motion of the molecules' center of mass.<sup>13</sup> The method, though, is sensitive to contaminants in the polymer, e.g., rapidly diffusing substances,<sup>13,14</sup> and is subject to misinterpretation of the results if the polymer is significantly polydisperse.<sup>14-16</sup>

Star-branched polymers, particularly those with arms of equal length, are the simplest systems allowing the study of branching.<sup>17,18</sup> In a previous PGSE study<sup>19</sup> we measured the self-diffusion of star-branched polyisoprenes as a function of  $f$ , the number of arms, over the full range of concentration in solvents. We found that in going from a linear ( $f = 2$ ) to a three-armed star ( $f = 3$ ) polyisoprene of equal arm size (hence 50% greater molecular weight), the difference in the diffusion constant in dilute solutions was within error still entirely attributable to the molecular weight change. Thus the difference in molecular dimensions due only to this change in architecture<sup>5,19,20</sup> was not evident for  $f < 4$ , although it was clearly evident for  $f = 8$  and  $f = 18$ .

The present study compares diffusivity for  $f = 2$  and  $f = 3$  in two other systems, polystyrene and polybutadiene, each over a molecular weight range covering some 2.5 orders of magnitude. Substantial differences between those polymers are found in the diffusivity and its concentration dependence in dilute  $\text{CCl}_4$  solutions over the entire range of molecular weight investigated. Again, the difference between  $f = 2$  and  $f = 3$  at the same total molecular weight is not significant. In fact, the two architectures will be seen to maintain their essentially identical behavior beyond the semidilute regime. Thus reptation,<sup>7,8</sup> with its expected profound differences between  $f = 2$  and  $f > 2$ , must be confined to more concentrated solutions and the melt even at our highest molecular weights. However, it is just under such conditions that the diffusivities approach the lower

Table I  
Molecular Parameters of Linear Polybutadienes

sample	$\bar{M}_n \times 10^{-4},^a$ dalton	$\bar{M}_w \times 10^{-4},^b$ dalton	$\frac{\bar{M}_z}{\bar{M}_w}^b$	$\frac{\bar{M}_w}{\bar{M}_n}^b$
CDS-B3	0.25	0.26	1.04	1.04
JK-6	0.29	0.31	1.04	1.05
WG-1	0.72	0.76	1.06	1.04
JK-4	0.89	0.92 <sup>c</sup>	1.04	1.03
JK-2	1.20	1.24	1.05	1.03
WG-4	4.10	4.31 <sup>c</sup>	1.03	1.05 <sup>d</sup>
WG-9	7.50	7.81 <sup>c</sup>	1.05	1.04 <sup>d</sup>
LF-4	9.01	9.60 <sup>c</sup>	1.07	1.07 <sup>d</sup>

<sup>a</sup> Via osmometry. <sup>b</sup> Via size exclusion chromatography; the columns were calibrated with polybutadiene standards prepared and characterized in these laboratories. <sup>c</sup> Via light scattering. <sup>d</sup> Via absolute measurements.

limits attainable with the PGSE method.<sup>15,19</sup> Moreover, the definition of diffusion provided by this method begins to depart, for very large molecules, from the pure center-of-mass motion of interest.<sup>13,19</sup> Our earlier work did, however, indicate<sup>19</sup> that, in the absence of entanglements, molecular motions for  $f = 3$ ,  $f = 8$ , and  $f = 18$  are not qualitatively different from those of linear polymers at any concentration, including the melt. For these reasons, the present work largely confines itself to the dilute and semidilute regimes. No evidence of multiple echo attenuation rates unrelated to contamination, nor of time-dependent diffusivities, was ever observed. The results are interpreted in terms of the theory of dilute solutions, with particular emphasis on scaling laws based on molecular weight. Preliminary reports of this work have been given.<sup>21</sup>

## Experimental Section

The preparation and characterization of the linear and star-shaped polystyrenes and polybutadienes followed the methods described elsewhere.<sup>17,22,23</sup> The anionic polymerization methods resulted in linear polymers of very low dispersity ( $\bar{M}_w/\bar{M}_n \leq 1.1$  in all cases). In the case of star molecules these become the arms to be linked, using methyltrichlorosilane. Repeated fractionation removed any remaining linear material. Thus the star molecules had a dispersity equal to or lower than the constituent arm material. Tables I-IV summarize the molecular characteristics of the resulting polymers. In the initial phases of the present work, small amounts of antioxidants had been added to the polybutadiene specimens. In each of these cases the PGSE experiments were repeated using polymer of the original batch without antioxidant; the final results in dilute solutions reflect only measurements on samples without antioxidant.

Polymer characterization was performed by using a combination of size exclusion chromatography (GPC), membrane osmometry, and light scattering. A Chromatix KMX-6 low-angle photometer

Table II  
Molecular Parameters of Three-Armed  
Star-Branched Polybutadienes

sample	$\bar{M}_n \times 10^{-4},^a$ dalton	$\bar{M}_w \times 10^{-4},^b$ dalton	$f^c$
JK-5A	0.65		3.05
JK-7A	0.67		2.97
JK-6A	0.87	0.89	2.97
WG-2AA	1.61		2.98
WG-1A	2.10		2.91
JK-4AA	2.60		2.92
JK-3A	2.90		2.90
WG-3A	7.60	7.74	3.04
WG-4A	12.3		3.00
WG-8AA	16.1	17.3	2.92
WG-9AA	22.7		3.03
WG-7AA	28.1	29.3	2.96

<sup>a</sup> Via osmometry. <sup>b</sup> Via light scattering. <sup>c</sup> Degree of branching:  $f = \bar{M}_n(\text{star})/\bar{M}_n(\text{arm})$ .

Table III  
Molecular Parameters of Linear Polystyrenes

sample	$\bar{M}_n \times 10^{-4},^a$ dalton	$\bar{M}_w \times 10^{-4},^b$ dalton	$\frac{\bar{M}_z}{\bar{M}_w}^c$	$\frac{\bar{M}_w}{\bar{M}_n}^d$
PS-101481	0.57	0.63	1.04	1.10
PS-12282A	1.79	1.90	1.03	1.06
PS-111281	2.10	2.16	1.04	1.05
PS-12382	4.30	4.31	1.04	1.00
PS-12282B	5.38	5.70	1.03	1.06
PS-3182	7.78	8.11	1.03	1.04 <sup>c</sup>
PS-2182A	12.7	13.0	1.04	1.03 <sup>c</sup>

<sup>a</sup> Via osmometry. <sup>b</sup> Via light scattering. <sup>c</sup> Via size exclusion chromatography. <sup>d</sup> Via absolute measurements.

Table IV  
Molecular Parameters of Three-Armed  
Star-Branched Polystyrenes

sample	$\bar{M}_n \times 10^{-4},^a$ dalton	$\bar{M}_w \times 10^{-4},^b$ dalton	$f^c$
3PS-3A	1.35	1.40	2.97
3PS-4AA	2.10	2.18	2.98
3PS-2A	2.92	3.00	2.92
3PS-1A	3.43	3.50	2.93
PS-B3	5.46	5.60	2.96
PS-D3	16.8	17.3	2.99
PS-J3		108.0	3.03 <sup>d</sup>

<sup>a</sup> Via osmometry. <sup>b</sup> Via light scattering. <sup>c</sup> Degree of branching:  $f = \bar{M}_n(\text{star})/\bar{M}_n(\text{arm})$ . <sup>d</sup>  $f = \bar{M}_w(\text{star})/\bar{M}_w(\text{arm})$ .

was used, as was a Waters 150C GPC. The 150C GPC had a six-column  $\mu$ -Styragel set with a porosity range of  $10^2$ – $10^6$  Å; the carrier solvent, THF, was used at a flow rate of 1 mL min<sup>-1</sup>. The temperature of measurement was 30 °C. The polybutadiene microstructure was examined by <sup>1</sup>H NMR. The polybutadienes used had the anticipated microstructure of ca. 36% cis-1,4, 57% trans-1,4, and 7% vinyl. The  $dn/dc$  values for the samples were determined<sup>24,25</sup> via the use of the Chromatix KMX-16 refractometer. Toluene was used for the polystyrenes while cyclohexane was used for the polybutadienes. Molecular parameters of all samples are given in Tables I–IV.

The solvent for the diffusion experiments was tetrachloromethane (CCl<sub>4</sub>) (Matheson Coleman and Bell, 99.5% pure, less than 0.01% H<sub>2</sub>O). Because polymer concentrations as low as 0.15 wt % were used, it was essential that no proton NMR be detectable in the pure solvent. Signal averaging was used to ensure that the proton signal from any solvent contaminants was not visible in the spin-echo (90°– $\tau$ –180° sequence,  $\tau = 25$  ms) at a signal-to-noise ratio greater than 0.1 per single pass. In the few instances where this condition was not satisfied, the contamination

was shown to originate on the walls of the solvent-transfer glassware, which was changed before preparing each series of samples. In these cases, new preparations were made.

Polymer materials were kept under vacuum at 40–60 °C for several weeks before the NMR samples were prepared in order to remove traces of absorbed water and other volatile components, i.e., solvents. CCl<sub>4</sub> solutions were prepared within the thin-walled 7-mm-o.d. NMR sample tubes, which were sealed under dry N<sub>2</sub> gas immediately after weighing to determine the final polymer concentration. For polymer concentrations below about 1 wt %, it was necessary to increase the precision of the concentration determination by preparing a larger batch of solution, a requisite amount of which was transferred into the sample tube after at least 24 h to obtain equilibrium concentration. Diffusion was measured at least twice during the period of 1 day to 6 weeks after preparation of the sample. No difference in diffusivity, or evidence of other changes, could be found during that time. Postanalysis GPC evaluations performed for some of the samples confirmed that the polymers had not undergone chain branching or degradation.

The Mark–Houwink relations for linear polybutadiene and polystyrene were determined in CCl<sub>4</sub> solution at 50 °C. This was done since no equations were available from the literature. The samples used were near-monodisperse materials prepared and characterized in this laboratory. The viscometers used were of the Cannon–Ubbelohde type having negligible kinetic energy corrections.

The PGSE apparatus<sup>13,26,27</sup> was based on a Spin-Lock Ltd. 33-MHz pulsed NMR spectrometer used to detect <sup>1</sup>H NMR in the 90°– $\tau$ –180° mode, with  $\tau$  typically 25 ms, except for measurements at high polymer concentrations and in the melt, where  $\tau = 50$  ms was used. A steady gradient of magnitude  $G_0 = 9 \times 10^{-3}$  T m<sup>-1</sup> was applied to narrow and stabilize<sup>28</sup> the spin echo, while gradient pulses of magnitude  $G = 1$ – $3$  T m<sup>-1</sup> and duration  $\delta = 0.1$ – $30$  ms provided the bulk of the echo attenuation. Data taking was performed with a dedicated microprocessor<sup>27</sup> which permitted signal averaging. The lowest usable polymer concentrations were approximately 0.15 wt % ( $\approx 2.5$  kg m<sup>-3</sup>), where the single-pass signal-to-noise ratio was approximately 3:1 for the unattenuated echo at  $\tau = 25$  ms. From 10 to 80 echoes were accumulated for each of about 8–15 values of  $\delta$  at fixed  $G$  and  $G_0$ , which permitted extraction of the diffusion coefficients  $D$  with a reproducibility of 1–2% (2–4% at the lowest concentrations). An additional uncertainty of 2–3% due to gradient calibration is in effect an unknown systematic error which does not enter into any comparisons among our data.

The diffusion coefficients were obtained from measurements of the echo height  $A$  as a function of  $X$  in the following way:<sup>10,26,29</sup>

$$A(X)/A(0) = \exp(-\gamma^2 DX) \quad (1)$$

where

$$X = \delta^2 G^2 (\tau - \delta/3) - GG_0 \delta [(t_1^2 + t_2^2) + \delta(t_1 + t_2) + 2/3\delta^2 - 2\tau^2]$$

with  $t_2 = \tau - t_1 - \delta$ ,  $t_1$  being the delay between radio-frequency and gradient pulses. The second term in  $X$  was nonnegligible at our highest diffusion coefficients and was always included in our analysis.

A batch computer program<sup>29</sup> based on least-squares curve fitting was used to extract  $D$  from the data ( $A \pm \Delta A$  vs.  $\delta$ ) and to test the applicability of the single-diffusivity model implied by eq 1. In a small fraction of cases, contamination was detected in this way and traced to a specific cause, e.g., antioxidant added to some polybutadienes but not to others. In these cases, the data were rejected, or only the appropriate diffusion coefficient was extracted from the data.

However, a difference in initial and final slopes (i.e.,  $D_{\max} > D_{\min}$ ) can also be caused by the polydispersity of the polymer. Since we routinely obtained a reduction of the echo height by a factor of 3–5 even at the lowest concentrations and by a factor of 10–20 above  $\sim 1$  wt % polymer, we were able to observe a small but significant curvature in the plot of  $\log A$  vs.  $X$ , even at the present small polydispersities. Therefore, eq 1 was modified as follows:<sup>14,16</sup>

$$A(X)/A(0) = \sum_i W(M_i) \exp[-2\tau/T_2(M_i)] \exp[-\gamma^2 D(M_i)X] \quad (2)$$

Table V  
 Polybutadiene Diffusion Results in CCl<sub>4</sub>

linear polybutadienes			star polybutadienes		
sample	log $D_0^a$	log $k_F^b$	sample	log $D_0^a$	log $k_F^b$
CDS-B3	-9.66 ± 0.02	-2.25 ± 0.05	JK-5A	-9.87 ± 0.02	-1.87 ± 0.05
JK-6	-9.70 ± 0.02	-2.36 ± 0.05	JK-7A	-9.85 ± 0.02	-1.97 ± 0.05
WG-1	-9.89 ± 0.02	-1.77 ± 0.05	JK-6A	-9.96 ± 0.02	-1.80 ± 0.05
JK-4	-9.94 ± 0.03	-1.70 ± 0.05	WG-2AA	-10.09 ± 0.03	-1.58 ± 0.05
JK-2	-10.07 ± 0.03	-1.76 ± 0.05	WG-1A	-10.17 ± 0.03	-1.57 ± 0.05
WG-4	-10.37 ± 0.04	-1.37 ± 0.06	JK-4AA	-10.25 ± 0.03	-1.42 ± 0.05
WG-9	-10.55 ± 0.04	-1.09 ± 0.06	JK-3A	-10.28 ± 0.04	-1.31 ± 0.06
LF-4	-10.59 ± 0.05	-1.10 ± 0.06	WG-3A	-10.49 ± 0.04	-1.17 ± 0.06
			WG-4A	-10.72 ± 0.05	-1.04 ± 0.06
			WG-8AA	-10.72 ± 0.04	-0.85 ± 0.07
			WG-9AA	-10.82 ± 0.04	-0.92 ± 0.07
			WG-7AA	-10.84 ± 0.05	-0.89 ± 0.07

<sup>a</sup>  $D_0$  in m<sup>2</sup> s<sup>-1</sup>. <sup>b</sup>  $k_F$  in m<sup>3</sup> kg<sup>-1</sup>.

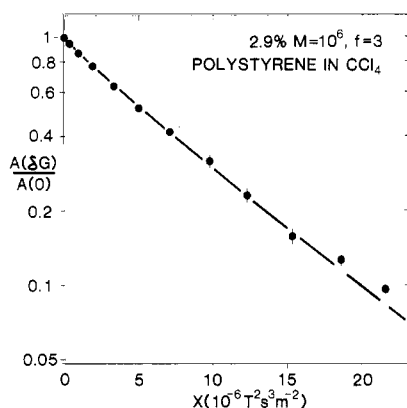


**Figure 1.** Normalized spin-echo height vs. gradient parameter  $X$  (see eq 1) for a sample of 2.9 wt % PS-J3 polystyrene (see Table IV) dissolved in CCl<sub>4</sub> at 50 °C. Solid line (slightly curved; see ref 16) represents fit of eq 2 to data.

It was possible to simulate the dependence of  $A$  on  $X$  and adjust a single scaling parameter,  $D(\bar{M}_n)$ , to obtain a least-squares fit to the data. The methods employed, and the computer program based on them, are described elsewhere.<sup>16</sup> All of our data from uncontaminated samples were reanalyzed in this manner, with a modest improvement in the  $\chi^2$  measure of goodness of the fit and a corresponding reduction in the (random) uncertainty in  $D(\bar{M}_n)$ . All diffusion coefficients reported in this work thus represent  $D(\bar{M}_n)$ , the diffusivities of molecules of molecular weight  $M = \bar{M}_n$ . Typical echo attenuation data and analysis via eq 2 are shown in Figure 1.

The ability of PGSE experiments to detect polydispersity and contamination was put to inadvertent use in one three-armed polybutadiene specimen in which the functionality  $f$  (see Table II) had been found to be 2.85. In this specimen two distinct diffusion coefficients, differing by a factor of about 2, were observed between 0.5 and 12 wt % polymer in CCl<sub>4</sub> solution. The GPC chromatogram showed a subsidiary peak near 1/3 the molecular weight of the star, i.e., the "parent" arm. Its size was consistent with the spin-echo fraction attributable to the fast-diffusing component, the observed  $f$ , and the diffusivity ratio. All evidence pointed to the existence of some 10% of unreacted arms in the polymer. This sample was, of course, not included in our work. However, the ease of observation of the rapidly diffusing component via PGSE, combined with the absence of comparable symptoms in any other sample, contributes to our confidence that unreacted arms, or molecules missing an arm, constitute less than 1 wt % of any of our polymers.

We found that heating the NMR sample tube some 12 cm above the sample volume to about 80 °C created an inverted temperature profile which suppressed convection<sup>30</sup> without causing a detectable temperature gradient in the sample liquid at 50 °C. This method was used routinely and successfully below 0.6 wt % polymer. No effects of convection could ever be detected at any higher concentration, even without active prevention.

## Results and Discussion

Measurements of self-diffusion of linear as well as three-armed star-branched polybutadiene and polystyrene molecules were performed at 50 °C, between about 0.15 wt % and at least 8 wt % in CCl<sub>4</sub> solution. For the lower molecular weight polymers the measurements could be performed across the full concentration range. In all cases the polymer self-diffusion rate decreased with increasing polymer concentration, the rate of decrease being highest at the largest molecular weights.

Our results for linear polystyrenes in most respects resemble those of Callaghan and Pinder<sup>11,12</sup> when the 22 °C temperature difference between their experiment and ours is taken into account. However, in no uncontaminated sample (including all polybutadienes and star polystyrenes) did we observe two-component diffusion, despite the fact that we routinely pursued echo attenuation to  $A(X)/A(0) \leq 0.1$  even in the dilute regime. Also, tests for a time dependence of diffusivity (by varying  $\tau$  between 8 and 100 ms) failed to find significant differences. Our largest polystyrene, a star (PS-J3,  $M \approx 10^6$ ; see Table IV) was no exception in this regard (see Figure 1; cf. ref 11).

Our observations in three-armed star polystyrenes are identical with those in the linear polystyrenes. Moreover, the results for polybutadienes, linear as well as star branched, are very similar to those for polystyrenes except for the slower diffusion at a given molecular weight and the greater rate of diffusivity decrease with concentration.

Diffusion behavior in the dilute regime can be characterized to first order in hydrodynamic terms analogous to those employed for sedimentation and viscosity:<sup>12,31</sup>

$$D^{-1}(c) = D_0^{-1}(1 + k_F c + \dots) \quad (3)$$

where  $D_0$  is the (extrapolated) trace diffusion constant,  $c$  being the concentration (polymer mass per solution volume). Both  $D_0$  and  $k_F$  can be determined from the initial linear region of a plot of  $D^{-1}$  vs.  $c$ . Figure 2 shows such plots for various polybutadienes of smaller molecular weights, with  $c$  restricted to below  $\sim 100$  kg m<sup>-3</sup>. The straight lines are least-squares fits to the data.  $D_0$  was obtained from the intercept, and  $k_F$  from the slope and intercept. These values are listed in Tables V and VI.

At higher molecular weights, the range of linear behavior became more restricted. Our observations in this regard generally agree with those of Callaghan and Pinder<sup>12</sup> for polystyrenes and are similar for polybutadienes except for small quantitative differences. Figure 3 shows typical data for the higher molecular weight polybutadienes. In order to obtain  $D_0$  and  $k_F$  in these cases, a straight line was fitted to data up to a concentration at which the Gauss criterion detects a termination of the linear regime within experi-

Table VI  
Polystyrene Diffusion Results in  $\text{CCl}_4$

linear polystyrenes			star polystyrenes		
sample	$\log D_0^a$	$\log k_F^b$	sample	$\log D_0^a$	$\log k_F^b$
PS-101481	$-9.75 \pm 0.03$	$-2.18 \pm 0.05$	3PS-3A	$-9.87 \pm 0.03$	$-1.89 \pm 0.05$
PS-12282A	$-9.91 \pm 0.03$	$-1.92 \pm 0.05$	3PS-4AA	$-9.96 \pm 0.03$	$-1.87 \pm 0.05$
PS-111281	$-9.98 \pm 0.03$	$-1.75 \pm 0.05$	3PS-2A	$-10.05 \pm 0.03$	$-1.73 \pm 0.05$
PS-12382	$-10.15 \pm 0.03$	$-1.49 \pm 0.05$	3PS-1A	$-10.10 \pm 0.03$	$-1.68 \pm 0.05$
PS-12282B	$-10.19 \pm 0.03$	$-1.56 \pm 0.05$	PS-B3	$-10.21 \pm 0.04$	$-1.61 \pm 0.07$
PS-3182	$-10.24 \pm 0.03$	$-1.45 \pm 0.05$	PS-D3	$-10.51 \pm 0.04$	$-1.33 \pm 0.07$
PS-2182A	$-10.39 \pm 0.03$	$-1.49 \pm 0.05$	PS-J3	$-10.8 \pm 0.1$	$-1.01 \pm 0.07$

<sup>a</sup>  $D_0$  in  $\text{m}^2 \text{s}^{-1}$ , <sup>b</sup>  $k_F$  in  $\text{m}^3 \text{kg}^{-1}$ .

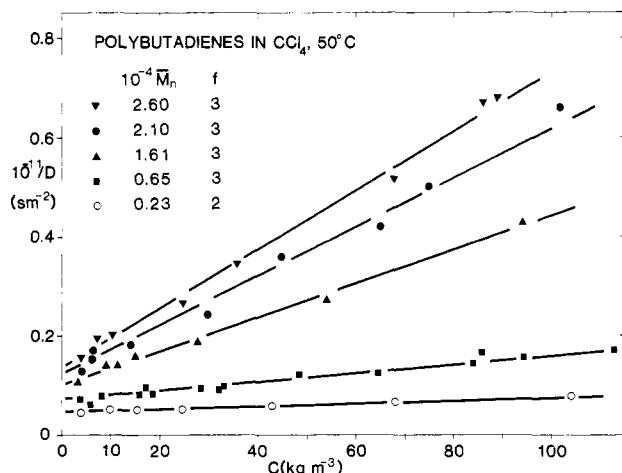


Figure 2. Inverse diffusivity vs. polymer concentration for several low molecular weight polybutadienes, linear and stars. Samples represented are (see Tables I and II) CDS-B3, JK-5A, WG-2AA, WG-1A, and JK-4AA. Straight lines are least-squares fits to data.

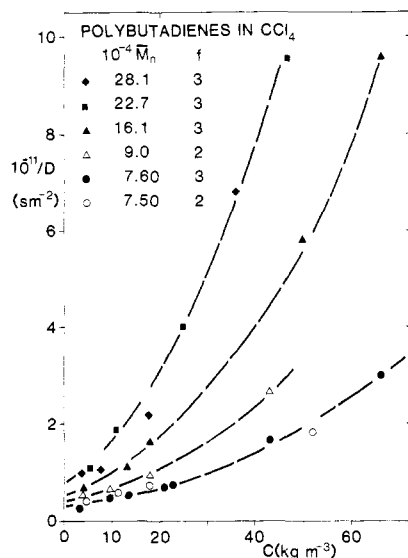


Figure 3. Inverse diffusivity vs. polymer concentration for some higher molecular weight linear and star polybutadienes. Samples represented (see Tables I and II) are WG-9, WG-3A, LF-4, WG-8AA, WG-9AA, and WG-7AA. Lines are hand drawn.

mental error. Plots of  $\log D$  vs.  $c$  at low  $c$  generally display only small curvature, so that  $D_0$  and  $k_F$  could also be obtained from those plots, with an appropriate transformation of eq 3. The values reported here were checked and occasionally supplemented in this manner.

Figure 4 shows log-log plots of  $D$  vs.  $c$ . For the smaller polybutadienes the data cover the full range of  $c$ . Our observations in polystyrenes, both linear and three armed, are very similar; for linear PS they agree at least semi-quantitatively with those of other workers.<sup>11,12,32</sup> de Gen-

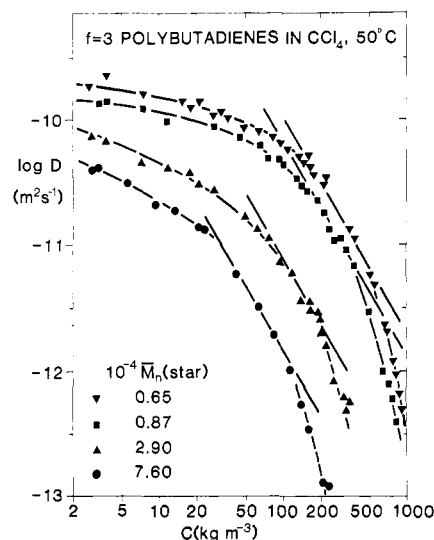
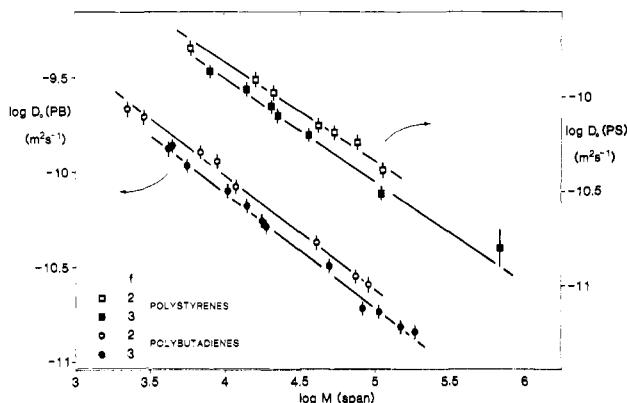


Figure 4. log-log representation of polybutadiene star diffusion constant vs. concentration in  $\text{CCl}_4$  solution. Samples shown (see Table II) are JK-5A, JK-6A, JK-3A, and WG-3A. Solid lines have slopes of  $-1.75$ ; dashed lines are hand-drawn smooth interpolations.

nes' prediction<sup>7</sup> of a concentration scaling regime  $D \propto c^{-1.75}$  ( $c^* < c < c^{**}$ ) is not borne out by our data for either polymer (both  $f = 2$  and  $f = 3$ ) at any molecular weight. The slopes of all our plots of  $\log D$  vs.  $\log c$  (e.g., Figure 4) change continuously, taking the value  $-1.75$  at some intermediate concentration which decreases with increasing  $M$ .

A molecular weight scaling law  $D \propto M^{-2}$  has also been predicted<sup>7</sup> for the semidilute regime. For polystyrene, indices of  $-1.4$  (in  $\text{CCl}_4$ , PGSE work<sup>11</sup>) and  $-2.05 \pm 0.1$  (in benzene, forced Rayleigh scattering<sup>32</sup>) have been found. The present experiment may be interpreted similarly by drawing tangents with slope  $-1.75$  to data  $\log D$  vs.  $\log c$  and evaluating their intercepts  $D'$  at  $c = 100 \text{ kg m}^{-3}$ . For our polybutadienes, plots of  $\log D'$  vs.  $\log M$  follow an excellent straight line with slope  $-1.76 \pm 0.08$ ; for polystyrenes, the scaling index is  $-1.7 \pm 0.1$ . These values, however, are suspect both because the semidilute concentration scaling regime on which they are based could not be demonstrated experimentally and because at the highest  $M$  (hence the lowest  $D$ ) segmental motions are probably beginning to contribute to the diffusivities measured via PGSE.<sup>13,32</sup> It has recently been suggested<sup>33,34</sup> that  $c^*$  as defined here represents the concentration associated with the onset of screening of the hydrodynamic interaction rather than the onset of entanglements, which should occur at a higher concentration and molecular weight. In that case, any scaling behavior observed in the semidilute regime is probably unrelated to reptation, even at molecular weights considerably higher than those of Figure 4.



**Figure 5.** Power-law representation of polymer diffusion coefficient at infinite dilution in  $\text{CCl}_4$  vs. span molecular weight. For linear polymers,  $M(\text{span}) = \bar{M}_n$ ; for three-armed stars,  $M(\text{span}) = 2\bar{M}_n/3$ . Each straight line is a least-squares fit to data of a single polymer and architecture. Two separate vertical scales are used to avoid clutter.

Figure 5 shows the molecular-weight dependence of  $D_0$  for all polymers listed in Tables I–IV. Since hydrodynamics in dilute solution depends on molecular size, the abscissa represents span molecular weight, where for linear ( $f = 2$ ) molecules  $M(\text{span}) = \bar{M}_n$ , while for three-armed stars ( $f = 3$ ),  $M(\text{span}) = 2\bar{M}_n/3$ . The choice of  $\bar{M}_n$  corresponds to our data reduction convention  $D \equiv D(\bar{M}_n)$  (see above). The use of  $\bar{M}_w$  instead of  $\bar{M}_n$  for both axes would simply shift all data by a small amount parallel to the fitted straight lines without affecting slope or intercept.

Each of the four sets of data is consistent with a simple power law

$$\log D_0 = A + s \log M \quad (4)$$

with the slopes  $s$  being within error equal for linear and star-branched molecules of a given species but significantly greater (negatively) for polybutadienes than for polystyrenes. However, plots of  $\log D_0$  vs.  $\log M(\text{total})$  are consistent with straight lines common to both architectures for a given polymer, with  $\chi^2$  per degree of freedom not significantly different from that for the respective individual fits shown in Figure 5. The slopes and intercepts are, of course, better defined in the fits to the combined data. The results are for all polystyrenes

$$\log D_0(\text{PS}) = (-7.743 \pm 0.006) - (0.52 \pm 0.01) \log M \quad (5a)$$

and for all polybutadienes

$$\log D_0(\text{PB}) = (-7.600 \pm 0.005) - (0.60 \pm 0.01) \log M \quad (5b)$$

with  $D_0$  in  $\text{m}^2 \text{s}^{-1}$ . These fits are shown with the replotted data in Figure 6.

The power-law slope for the polystyrenes in  $\text{CCl}_4$  is in agreement with earlier work,<sup>12</sup> while the difference in intercepts is accounted for by our use of 50 °C as working temperature. The magnitudes of the slopes suggest that  $\text{CCl}_4$  is a substantially better solvent for polybutadiene than for polystyrene.

The indistinguishability between linear and three-armed star molecules of the same species at the same molecular weight encompasses  $k_F$  (see below) as well as  $D_0$  and seems to extend into and beyond the semidilute regime (see Figure 4). Thus the PGSE experiment is not sensitive enough to detect the relatively subtle difference in  $D_0$  between  $f = 2$  and  $f = 3$  at equal  $M$  predicted by theories.<sup>3,4,20</sup> It amounts to some 5%, roughly commensurate with the precision in the differences between the appro-

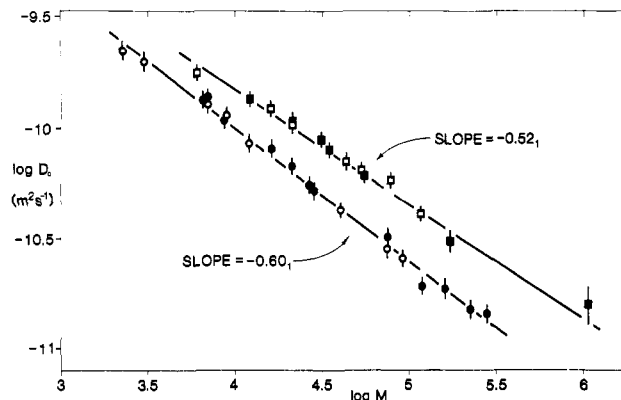


**Figure 6.** Data of Figure 5 replotted vs.  $\log \bar{M}_n$ . Single straight lines are fitted to each polymer type irrespective of architecture.

appropriate intercepts in Figure 5.

The molecular-weight dependence of polymer diffusivity at infinite dilution may be explained in terms of Flory's theory of dilute solutions,<sup>2</sup> according to which<sup>15</sup>

$$D_0 = \frac{kT}{\eta_0 P} \frac{1}{\alpha} M^{-0.5} \left[ \frac{M}{\langle S^2 \rangle} \right]^{0.5} \quad (6)$$

where  $P$  is a numerical constant,  $\eta_0$  represents the solvent viscosity,  $k$  is Boltzmann's constant, and  $T$  is the absolute temperature. The term in the square brackets is essentially independent of  $T$  and  $M$  and is a characteristic of a given polymer and architecture. The distinction between  $f = 2$  and  $f = 3$  can be ignored here (see above). The quantity  $\alpha$  describes the solvent power and is related to intrinsic viscosity:<sup>2</sup>

$$[\eta] = [\eta]_0 \alpha^3 \quad (7)$$

Measurements under  $\Theta$ -conditions are available from the literature. For polystyrenes<sup>35,36</sup>

$$[\eta]_0 = 8.4 \times 10^{-5} \bar{M}_w^{0.50} \text{ m}^3 \text{ kg}^{-1} \quad (8a)$$

whereas for anionic polybutadienes<sup>37</sup>

$$[\eta]_0 = 1.78 \times 10^{-4} \bar{M}_w^{0.50} \text{ m}^3 \text{ kg}^{-1} \quad (8b)$$

In order to use eq 7 to determine  $\alpha$ , measurements of  $[\eta]$  for linear polymers of both species in  $\text{CCl}_4$  at 50 °C were performed. The results are given in Table VII.

A least-squares power-law fit to the molecular-weight dependence of  $[\eta]$  yields, for polystyrene and polybutadiene, respectively:

$$[\eta]_{\text{PS}} = (1.53 \pm 0.08) \times 10^{-5} \bar{M}_w^{0.694 \pm 0.006} \quad (9a)$$

$$[\eta]_{\text{PB}} = (1.79 \pm 0.08) \times 10^{-5} \bar{M}_w^{0.782 \pm 0.005} \quad (9b)$$

both in  $\text{m}^3 \text{ kg}^{-1}$ . Solving eq 7–9 for  $\alpha$  yields

$$\alpha(\text{PS in } \text{CCl}_4, 50^\circ \text{C}) = (0.57 \pm 0.01) \bar{M}_w^{0.065 \pm 0.005} \quad (10a)$$

$$\alpha(\text{PB in } \text{CCl}_4, 50^\circ \text{C}) = (0.47 \pm 0.01) \bar{M}_w^{0.094 \pm 0.005} \quad (10b)$$

Substitution into eq 6 now results in a prediction for the molecular-weight dependences of  $D_0$ , for comparison with the experimental results, eq 5. In the notation of eq 4, the power-law slopes  $s$  in Figure 6 would be expected to be

$$s_{\text{PS}} = -0.565 \pm 0.005 \quad (11a)$$

$$s_{\text{PB}} = -0.594 \pm 0.005 \quad (11b)$$

Equation 11b is in agreement with observation for polybutadienes as expressed by eq 5b. However, the observed

Table VII  
Molecular Characteristics and Intrinsic Viscosities of Linear Polybutadienes and Polystyrenes

sample	$\bar{M}_n \times 10^{-4},^a$ dalton	$\bar{M}_w \times 10^{-4},^b$ dalton	$\frac{\bar{M}_z}{\bar{M}_w}^c$	$\frac{\bar{M}_w}{\bar{M}_n}^c$	$[\eta],$ $\text{m}^3 \text{kg}^{-1}$
Polybutadiene					
LF-2	2.1	2.20	1.03	1.04	0.0438
N-285	6.3	6.50	1.04	1.04	0.0982
LF-9	9.2	9.60	1.03	1.04	0.1500
LF-12	17.2	18.5	1.04	1.06	0.2320
LF-6	47.4 <sup>f</sup>	52.2	1.07	1.09	0.5251
LF-10		70.6	1.04	1.01	0.6658
Polystyrene					
111281	2.10	2.16	1.01	1.04	0.0147
11682	4.7	5.03	1.05	1.03	0.0285
S-102-M <sup>d</sup>	7.3	7.50	1.03	1.04	0.0386
2182A	12.7	13.0	1.05	1.06	0.0548
62382	15.0	15.8	1.04	1.05	0.0610
NBS-705	17.1 <sup>e</sup>	17.9 <sup>e</sup>	1.06	1.06	0.0675
L-11	20.2 <sup>f</sup>	20.8	1.01	1.09	0.0733
L-12	41.6 <sup>f</sup>	41.8	1.05	1.07	0.1169

<sup>a</sup> Membrane osmometry. <sup>b</sup> Low-angle laser light scattering; static mode. <sup>c</sup> Waters 150C GPC. <sup>d</sup> Fraction of Dow S-102 polystyrene standard. <sup>e</sup> Molecular weights determined by the National Bureau of Standards. <sup>f</sup> Via Waters 150C GPC-Chromatix KMX-6 combination.

exponent for polystyrenes is significantly different from that predicted via intrinsic viscosities. Such discrepancies are common in imperfect solvents and have been attributed<sup>38</sup> to spatial crossover effects, which affect  $D_0$  and  $[\eta]$  in different ways.

It should be pointed out that the Mark-Houwink exponent (e.g., in eq 9) determined by intrinsic viscosity experiments is known to undergo systematic decreases<sup>36</sup> below  $M \approx 3 \times 10^4$ . For this reason intrinsic viscosity measurements (Table VII) were performed only above  $M \approx 2 \times 10^4$ , whereas our diffusion experiments are approximately centered on that value. Omission of data for  $\log M \leq 4.5$  doubled the uncertainties in the determination of the slopes without significantly changing them. Thus we conclude that inclusion of the low-molecular-weight data in the computation of the slopes of Figure 6 may not be the source of the disagreement between eq 5a and 11a, and we include all data to retain full precision in eq 5.

Absolute magnitudes of the quantity  $M/\langle S^2 \rangle$  obtained via eq 6 are felt not to be sufficiently reliable. However, in computing their ratio between the two polymers, most of the systematic uncertainties cancel. Near the center of the molecular weight range covered by our experiments we thus obtain the ratio

$$\frac{[\langle S^2 \rangle / M]_{\text{PS in CCl}_4}}{[\langle S^2 \rangle / M]_{\text{PB in CCl}_4}} = 0.46 \pm 0.05 \quad (12)$$

Its value may be compared to the ratio of unperturbed molecular sizes on the basis of literature values<sup>37,39</sup> of the characteristic ratios,  $C_\infty$ , given appropriate bond lengths  $l$  and numbers of main-chain bonds at a common molecular weight,  $n_M$ :

$$\frac{\langle r_0^2(M) \rangle_{\text{PS}}}{\langle r_0^2(M) \rangle_{\text{PB}}} = \frac{[C_\infty l^2 n_M]_{\text{PS}}}{[C_\infty l^2 n_M]_{\text{PB}}} = 0.56 \quad (13)$$

Quantitative agreement with eq 12 cannot be expected since the latter involves modest molecular weights and a good solvent whose solvent power differs for the two polymers.

The concentration dependence of the polymer diffusion constant in the dilute regime is described by  $k_F$  in eq 3. It was determined from the slope and intercept of a straight-line fit to the data  $D^{-1}$  vs.  $c$  at the lowest con-

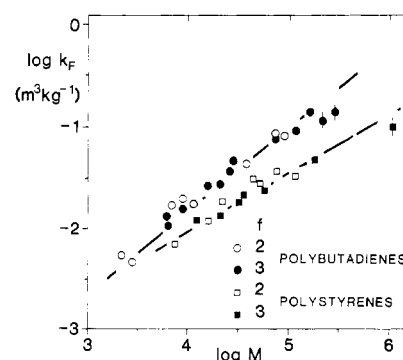


Figure 7. Initial concentration dependences ( $k_F$ ) of the polymer diffusivities (see eq 3 and Figures 2 and 3) as a function of molecular weight. Solid lines represent least-squares fits of straight lines to data.

centrations. The values of  $k_F$  for all samples described in Tables I and II are shown in Figure 7. Again, linear and three-armed star-branched molecules of the same polymer fall on the same curves, in both cases consistent with a straight line in a log-log plot. As in the case of  $D_0$ , different slopes and intercepts are found for the two polymers. The results of least-squares fits to the data of Figure 7 are

$$k_F(\text{PS}) = (4.8 \pm 0.2) \times 10^{-5} M^{0.57 \pm 0.02} \quad (14a)$$

$$k_F(\text{PB}) = (8.5 \pm 0.3) \times 10^{-6} M^{0.80 \pm 0.02} \quad (14b)$$

with  $k_F$  in  $\text{m}^3 \text{kg}^{-1}$ . The  $M$  dependence of  $k_F$  can also be predicted from intrinsic viscosities:<sup>40,41</sup>

$$k_F = 0.75[\eta] \quad (15)$$

With  $[\eta]$  given by eq 9, quantitative agreement with eq 14 is not obtained. In the case of polybutadienes, the exponent of  $M$  nearly agrees but the predicted  $k_F$  is some 14% too small at  $M = 3 \times 10^4$ . In the case of polystyrenes, the exponent of  $M$  is in disagreement with eq 14; the reason may be connected with the inclusion of low-molecular-weight data in the diffusion measurements (see discussion above). The value of  $k_F$  predicted by eq 15 with eq 9a at  $M = 3 \times 10^4$  exceeds the measurement, eq 14a, by 31%.

As might be expected, the agreement is more satisfactory in a correlation of results ( $D_0$  and  $k_F$ ) based purely on diffusion measurements, e.g., as permitted by the Pyun-

Fixman model<sup>4</sup> of dilute solutions. As elaborated by King et al.<sup>31</sup> this model may be expressed in the form

$$k_F = k_F^\phi \frac{NV_h}{M} \quad (16)$$

where  $V_h = (4\pi/3)(kT/6\pi\eta D_0)^3$ ,  $N$  being Avogadro's number. When eq 4 is substituted into eq 16, it is evident that the data in Figure 7 should follow the form

$$\log k_F = B - (3s + 1) \log M \quad (17)$$

with  $s$  having the values given in eq 5. The resulting slopes  $(-3s - 1)$  are  $0.56 \pm 0.02$  for polystyrene and  $0.80 \pm 0.02$  for polybutadiene, in excellent agreement with the measured exponents of  $M$  in eq 14. The intercepts  $B$  can also be calculated from eq 16 with eq 5, but the value of  $k_F^\phi$  is not precisely known except that it should be confined within the limits<sup>31</sup>  $2.23 \leq k_F^\phi \leq 7.16$ . The straight-line fit to the data of Figure 7 thus amounts to a determination of  $k_F^\phi$ . When the experimental uncertainty in  $s$  (eq 5) is propagated to eq 17 and, together with the uncertainty in  $B$ , to eq 16, the values of  $k_F^\phi$  for the two polymer species are found not to be significantly different, falling toward the lower end of the permissible region. Thus the Pyun-Fixman model provides a consistent description of our diffusion results in dilute solutions.

No measurements of  $A_2$  were available; however, the Yamakawa model<sup>3,31</sup> predicts a substantially steeper slope of  $\log k_F$  vs.  $\log M$  than observed (Figure 7) in both polymers if  $A_2$  comes (as is likely) even within an order of magnitude of the value<sup>31</sup> for polystyrene in 2-butanone at 25 °C.

### Concluding Remarks

The PGSE method of measuring self-diffusion of polymers in dilute and semidilute solutions determines center-of-mass motion of individual molecules so long as the diffusion distance  $d$  is sensibly greater than the coiled dimension of each molecule. Since

$$d = (2Dt)^{1/2} \quad (18)$$

with  $t \approx 100$  ms for PGSE,<sup>10,13,19</sup> it is easy to show that in our work this condition was not violated at  $c \lesssim c^*$  for any  $M$ , and at concentrations  $c \lesssim c^{**}$ , at least for  $M < 10^5$ . Since our search for multicomponent, cooperative, and non-Fickian diffusion phenomena was fruitless after a host of contamination and dispersity effects had been disposed of, it appears that polybutadienes and polystyrenes in  $\text{CCl}_4$  solution display relatively orthodox hydrodynamic behavior. Flory's dilute solution theory is a good guide to the infinite-dilution limit, with  $\text{CCl}_4$  constituting a "good" solvent for polybutadiene but not for polystyrene. The Pyun-Fixman model adequately predicts the molecular-weight dependence of  $k_F$ , although the postulated relation<sup>40,41</sup> between  $k_F$  and intrinsic viscosity is also useful. The difference between dilute polystyrene and polybutadiene diffusion rates at equal  $M$  appears to be mainly due to the difference in coiled molecular size at any given molecular weight.

The indistinguishability between linear and three-armed star molecules in dilute solutions is consistent with theory given our experimental uncertainties. In semidilute and concentrated solutions the same state of affairs is in accord with the view<sup>33,34</sup> that, in the presence of hydrodynamic screening but without entanglements or reptation, polymer intermolecular friction is mainly governed by the monomeric friction constant and the degree of polymerization.

However, work presently in progress indicates that significant differences in  $D_0$  as well as  $k_F$  exist between four- and six-armed polyisoprene stars of equal molecular

weight, as well as among polymethacrylates of the same molecular weight but different main-chain lengths vs. side-chain length and number. Thus PGSE investigation can serve as a useful supplement to intrinsic viscosity measurement in describing the influence of molecular architecture on hydrodynamics in solution. Provided that center-of-mass motion can be shown to be measured and provided the diffusion coefficient is not below  $D \approx 5 \times 10^{-14} \text{ m}^2 \text{ s}^{-1}$  (the practical limit for precise measurements), this usefulness can extend to melts and entangled systems. Under those circumstances the PGSE method can be used to investigate systems in which reptation may occur.

**Acknowledgment.** We thank B. Costarello and D. Thompson for their help with the preparation of the NMR samples and Xu Zhongde for several fruitful discussions about dilute solution hydrodynamics. We are also grateful to Prof. J. D. Ferry for several particularly illuminating comments. This work was supported by grants from the Polymers Program of the National Science Foundation (Grant DMR-79-08299), the Petroleum Research Fund, administered by the American Chemical Society, and the Faculty Research Committee of the University of Akron (Grant RG720).

**Registry No.** Polystyrene (homopolymer), 9003-53-6; polybutadiene (homopolymer), 9003-17-2; tetrachloromethane, 56-23-5.

### References and Notes

- (1) (a) Department of Physics, University of Akron. (b) The Institute of Polymer Science, University of Akron. (c) University of Athens; visiting scientist at The Institute of Polymer Science.
- (2) Flory, P. J. "Principles of Polymer Chemistry"; Cornell University Press: Ithaca, NY, 1953; Chapter 14.
- (3) Yamakawa, H. "Modern Theory of Polymer Solutions"; Harper and Row: New York, 1971.
- (4) Pyun, C. W.; Fixman, M. *J. Chem. Phys.* **1964**, *41*, 937.
- (5) Stockmayer, W. H.; Fixman, M. *Ann. N.Y. Acad. Sci.* **1953**, *57*, 334.
- (6) Yamakawa, H. *J. Chem. Phys.* **1962**, *36*, 2995.
- (7) de Gennes, P.-G. *Macromolecules* **1976**, *9*, 587, 594.
- (8) Doi, M.; Edwards, S. F. *J. Chem. Soc., Faraday Trans. 2* **1978**, *74*, 1789, 1802, 1818; **1979**, *75*, 38.
- (9) Roots, J.; Nyström, B.; Sundelöf, L.-O.; Porsch, B. *Polymer* **1979**, *20*, 337 and references cited therein.
- (10) Tanner, J. E. Ph.D. Thesis (Chemistry), University of Wisconsin, 1966.
- (11) Callaghan, P. T.; Pinder, D. N. *Macromolecules* **1980**, *13*, 1085.
- (12) Callaghan, P. T.; Pinder, D. N. *Macromolecules* **1981**, *14*, 1334.
- (13) von Meerwall, E.; Grigsby, J.; Tomich, D.; Van Antwerp, R. *J. Polym. Sci., Polym. Phys. Ed.* **1982**, *20*, 1037.
- (14) McCall, D. W.; Huggins, C. M. *Appl. Phys. Lett.* **1965**, *7*, 153.
- (15) Tanner, J. E.; Liu, K. J.; Anderson, J. E. *Macromolecules* **1971**, *4*, 586.
- (16) von Meerwall, E. *J. Magn. Reson.* **1982**, *50*, 409.
- (17) Bauer, B. J.; Fetters, L. J. *Rubber Rev.* **1978**, *51*, 406.
- (18) Bywater, S. *Adv. Polym. Sci.* **1979**, *102*, 2410.
- (19) von Meerwall, E.; Tomich, D. H.; Hadjichristidis, N.; Fetters, L. J. *Macromolecules* **1982**, *15*, 1157.
- (20) Mazur, J.; McCrackin, F. *Macromolecules* **1977**, *10*, 326.
- (21) Grigsby, J.; Tomich, D. H.; von Meerwall, E.; Fetters, L. J. *Bull. Am. Phys. Soc.* **1983**, *28*, 904.
- (22) Morton, M.; Fetters, L. J. *Rubber Rev.* **1975**, *48*, 359.
- (23) Khasat, N. Ph.D. Thesis (Polymer Science), University of Akron, 1982.
- (24) Hadjichristidis, N.; Fetters, L. J. *J. Polym. Sci., Polym. Phys. Ed.* **1982**, *20*, 2163.
- (25) Chen, N.; Xu, Z.; Carella, J.; Fetters, L. J.; Hadjichristidis, N.; Graessley, W. W., to be submitted.
- (26) von Meerwall, E.; Ferguson, R. D. *J. Appl. Polym. Sci.* **1979**, *23*, 877, 3657.
- (27) von Meerwall, E. *J. Magn. Reson.* **1979**, *34*, 339.
- (28) Hrovat, M. I.; Wade, C. G. *J. Magn. Reson.* **1981**, *44*, 62; **1981**, *45*, 67.
- (29) von Meerwall, E. *Comput. Phys. Commun.* **1979**, *17*, 309.
- (30) Kessler, D.; Weiss, A.; Witte, M. *Ber. Bunsenges. Phys. Chem.* **1967**, *71*, 3.
- (31) King, T. A.; Knox, A.; McAdam, J. D. G. *Polymer* **1973**, *14*, 293.



- (32) Léger, L.; Hervet, H.; Rondelez, F. *Macromolecules* 1981, 14, 1732.  
 (33) Amis, E. J.; Janmey, P. A.; Ferry, J. D.; Yu, H. *Polym. Bull.* 1981, 6, 13.  
 (34) Ferry, J. D., private communication.  
 (35) Roovers, J.; Bywater, S. *Macromolecules* 1972, 5, 384.  
 (36) Altares, T. A., Jr.; Wyman, D. P.; Allen, V. R. *J. Polym. Sci., Part A-2* 1964, 2, 4533.  
 (37) Hadjichristidis, N.; Xu, Z.; Fetters, L. J.; Roovers, J. *J. Polym. Sci., Polym. Phys. Ed.* 1982, 20, 743.  
 (38) Weill, G.; des Cloizeaux, J. *J. Phys. (Paris)* 1979, 40, 99.  
 (39) Brandrup, J.; Immergut, E. H., Eds. "Polymer Handbook", 2nd ed.; Wiley: New York, 1975.  
 (40) Mulderije, J. J. H. *Macromolecules* 1980, 13, 1207.  
 (41) Muthukumar, M. *J. Chem. Phys.* 1983, 78, 2764. Muthukumar, M.; DeMeuse, M. *Ibid.* 1983, 78, 2773.

## On Entanglements of Flexible and Rodlike Polymers

Shaul M. Aharoni

Corporate Research and Development, Allied Corporation, Morristown, New Jersey 07960.  
 Received November 17, 1982

**ABSTRACT:** Values of  $N_c$ , the number of chain atoms between "entanglements", were obtained for 62 flexible, semiflexible, and rodlike polymers and plotted against the corresponding values of the characteristic ratio  $C_\infty$  or the Kuhn step length  $A$ . It was found that the polymers are nicely divisible into the three groups above. Despite some scatter, the flexible polymers fall in a band about a line described by  $N_c \propto C_\infty^2$  or  $N_c \propto A^2$  and more specifically,  $N_c \cong 10C_\infty^2$  or  $N_c \cong (2.5 \text{ \AA}^{-2})A^2$ . In the case of rodlike polymers, the exponential dependence is less than 1.0, but the scatter prevents closer approximations. The semiflexible polymers fall in between the two extreme classes. When  $L_c$ , the chain length between "entanglements", is plotted against  $C_\infty$  or  $A$ , again a  $L_c \propto C_\infty^2$  or  $L_c \propto A^2$  relationship is obtained for flexible polymers. However, when  $R_c$ , the spatial distance between "entanglements" of flexible chains, is plotted, then relationships of the form  $R_c \propto C_\infty$  or  $R_c \propto A$  are obtained. The observations are discussed in terms of the "entanglements" being interferences to the translational and rotational mobility of whole rodlike molecules or whole or large parts of flexible macromolecules. The empirical relationships for flexible polymers indicated above are in excellent agreement with recent theoretical expectations in the literature.

### Introduction

"Entanglements" appear in molten bulk or highly concentrated solutions of long-chain molecules when these are forced by external force out of their state of equilibrium. In the case of flexible polymers, topological "entanglements" may serve as a valid model, but in the case of rodlike macromolecules, where apparent "entanglements" become manifest in relatively dilute, isotropic solutions, the physical meaning of "entanglements" remains obscure. In the case of rigid-rod polymers, the change in macroscopic behavior conventionally associated with the onset of entangled behavior may better be described in terms of concentration-dependent onset of interference to the free rotational and translational movement of the long rodlike molecules, reflected in rather abrupt decrease in their diffusion constants and an increase in solution viscosity. The interference with free movement, both rotational and translational, of flexible<sup>1-5</sup> as well as rodlike<sup>6-9</sup> chains was recently explained in terms of the reptation model. Comparisons of expectations based on the reptation theory with experimental results now appear in rapid succession. Several pertinent examples are given in ref 10-13.

Besides efforts directed at understanding the physical meaning of "entanglements", which will not be addressed in this work, the question arises as to the reason for the uniqueness to each undiluted polymer of the characteristic molecular weight between "entanglements",  $M_c$ , or the corresponding characteristic number of chain backbone atoms,  $N_c$ . Dilution of high molecular weight,  $M$ , polymers with  $M \gg M_c$ , does not significantly affect the "entanglement" interaction between polymer chains, as it was experimentally observed<sup>14</sup> that the onset of entangled behavior at a concentration  $c$  is well approximated by

$$(cM)_c \cong M_c \quad (1)$$

where  $(cM)_c$  is the product of concentration and molecular

weight at the point of onset of entangled behavior.

Based on the model of topological "entanglements", several empirical attempts were made in recent years to correlate  $M_c$  or  $N_c$  with some structural parameters of flexible polymers. The most extensive compilations of data assembled for such correlations are those of Boyer and Miller,<sup>15-20</sup> Privalko and Lipatov,<sup>21-25</sup> and Aharoni.<sup>26-28</sup> A comparison of these references reveals that the approaches adopted by the different authors are fundamentally similar to each other even though some scatter of data points and deviations from expectations exist. We believe that the choice of

$$M_c = 2M_e \quad (2)$$

is a contributing factor to the data scatter, besides the effects of heavy pendant atoms or groups on the correspondence of  $M_c$  to  $N_c$ . Here,  $M_e$  is the molecular weight between "entanglements" as obtained from the plateau modulus  $G_N^0$  of the polymer:<sup>29</sup>

$$G_N^0 = cRT/M_e \quad (3)$$

with  $R$  being the molar gas constant and  $T$  the absolute temperature. Allowing more accurate ratios of  $M_c/M_e$  (usually slightly over 2.0) to be used in the calculations of  $M_c$  and  $N_c$  from  $M_e$  undoubtedly will reduce the scatter of the data. However, due to the paucity of such precise data and in light of the fact that the large majority of  $M_c$  and  $N_c$  data assembled in this work were obtained from viscosity data of melts or concentrated solutions, all values of  $M_c$  obtained from  $M_e$  will be calculated according to eq 2 in order to maximize the number of evaluated polymers. In light of the results shown below, we do not believe that the data scatter significantly affects observed trends. In fact, attaching error bars of  $\pm 50\%$  to  $N_c$  values in Table I did not affect the trends seen in Figures 1-6. Because they so clutter the picture, the error bars were omitted from the figures.